

# Investigating the effects of contacting functional oxide films

K J O'Shea<sup>1</sup>, N Homonnay<sup>2</sup>, G Schmidt<sup>2</sup> and D A MacLaren<sup>1,3</sup>

<sup>1</sup>SUPA School of Physics and Astronomy, University of Glasgow, G12 8QQ, UK

<sup>2</sup>Fachbereich Physik, Martin-Luther-Universität Halle-Wittenberg, Halle (Saale), Germany

E-mail: dmaclaren@physics.org

**Abstract.** Advanced oxides are the current focus of intense research activity, driven by their numerous attractive properties for next generation microelectronics. However, reliable strategies must be developed for the electrical contacting of such films without compromising their functionality. We explore the effect of depositing both noble and oxidising metals onto the ferromagnetic  $\text{La}_{0.7}\text{Sr}_{0.3}\text{MnO}_3$  (LSMO) in terms of its structural and magnetic properties. Whilst noble metal overlayers have negligible impact, the metals typically used as adhesion layers, such as Ti, can drive a structural phase transition in the LSMO, producing a Brownmillerite phase and impairing the magnetisation.

## 1. Introduction

Functional oxides are promising candidates for next generation microelectronics owing to their wide range of ferroelectric, ferromagnetic and potential emergent interfacial properties such as interfacial superconductivity (within heterostructures) [1]. In addition to room temperature spintronic applications, functional oxides are also highly valuable in the investigation of spin dynamics [2] where the principal focus lies at the interface between ferromagnetic oxides and metals. Critically, all metal-oxide systems rely on smooth interfaces, good electrical contact and a lack of interfacial chemical reactions, therefore a complete understanding of the metallisation of functional oxides is essential for metal-oxide hybrid devices to be fully realised.

Here, we present a systematic study of the magnetic and structural effects of depositing metal contacts onto  $\text{La}_{0.7}\text{Sr}_{0.3}\text{MnO}_3$  (LSMO) thin films using transmission electron microscopy (TEM) and superconducting quantum interference device (SQUID) magnetometry. We find that complete quenching of the magnetisation of >10 nm oxide can occur after the deposition of just ~1 nm of a reducing metal. This degradation is important in the context of forming reliable metal contacts to functional oxides, especially where adhesion layers such as titanium are conventionally used.

## 2. Experiment Details

Pulsed laser deposition (PLD) [3] was used for epitaxial growth of LSMO, using (100)-oriented  $\text{SrTiO}_3$  (STO) substrates and stoichiometric polycrystalline targets. The PLD system employed a KrF excimer (248 nm) laser and the growth was monitored in-situ by high pressure reflection high energy electron diffraction (RHEED) [4]. Ten nanometre and 20 nm thick LSMO films were deposited using

<sup>3</sup> To whom any correspondence should be addressed.



a laser fluence of 2 - 3 J/cm<sup>2</sup>, a repetition rate of 5 Hz, an O<sub>2</sub> atmosphere of 0.2 mbar and a substrate temperature of 700°C. Following deposition of the oxide layer(s), samples were transferred to the electron beam evaporation chamber under UHV for deposition of the metals.

Scanning transmission electron microscopy (STEM) was used for structural characterisation of the metallised films and was performed on a JEOL ARM 200cF instrument. Electron energy loss spectroscopy (EELS) was used for chemical analysis of the interfaces and was conducted using a Gatan Quantum 965 spectrometer, typically using a dispersion of 0.5 eV/channel.

### 3. Results

Figure 1 provides an overview of the effect of depositing Au, Pt, Cu, CoFe, Cr and Ta electrical contacts on the crystal structure of LSMO films. Figures 1a and b are high angle annular dark field (HAADF) images of an LSMO film with a gold and platinum capping layer, respectively, with the Au/Pt layer appearing brightest. There are no discernible effects on the LSMO crystal structure resulting from the deposition of either Au or Pt (figures 1a,b), which is perhaps unsurprising given that neither of these elements is particularly reactive. SQUID measurements (figure 1g) indicate no substantial reduction in the magnetic moment of the LSMO with either a gold or platinum cap. In contrast, the SQUID measurements indicate a slight reduction in magnetic moment for a Cu contact and the LSMO crystal structure appears more diffuse (figure 1c), with a dark narrow band of intensity appearing at the Cu/LSMO interface in HAADF imaging. Similarly, the deposition of both Cr and Ta (figures 1e,f) produce a more prominent dark interfacial band and an almost complete loss of magnetisation. In each case, the dark band is consistent with the formation of an interfacial oxide, with the prospect of yielding an electrically insulating barrier layer between metal and LSMO.

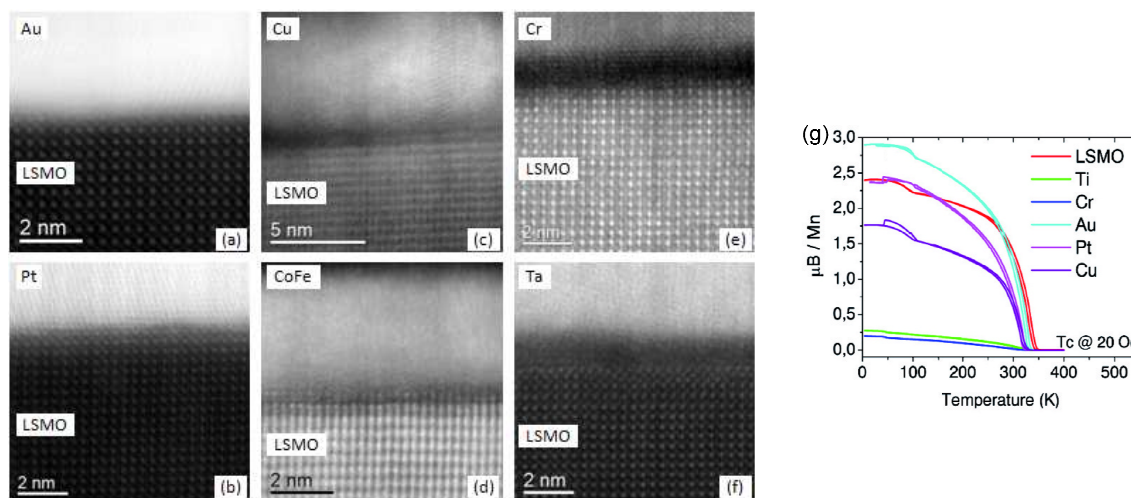


**Figure 1.** High angle annular dark field (HAADF) image summary of the effect of different metal contacts on LSMO films: (a) Au, (b) Pt, (c) Cu, (d) CoFe, (e) Cr and (f) Ta. There are no discernible effects for Pt and Au, however a significant interface region forms in the cases of Cu, CoFe, Cr and Ta, all of which are commonly used as electrical contacts or (for CoFe) magnetic contacts. SQUID measurements (f) indicate a substantial reduction in magnetisation following the deposition of Ti and Cr compared to the uncoated LSMO (red trace), whilst Cu reduces the magnetisation slightly and Au and Pt have no detrimental effect. The apparent increase in magnetization upon Au deposition is ascribed to sample-to-sample variations in LSMO quality.

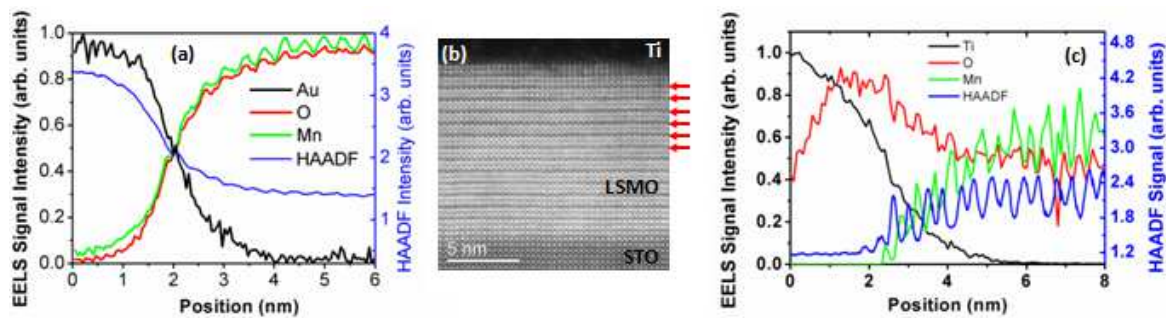


**Figure 2.** (a) EELS signal profiles of the Au (black), O (red) and Mn (green) across the LSMO/Au interface given in figure 1a, acquired using the Dual EELS [5] and spectrum imaging [6] methodologies within Digital Micrograph™ software. The HAADF signal intensity (blue) is also included for comparison. (b) HAADF image of the effect of Ti deposition onto LSMO. Red arrows highlight dark lattice planes which appear at a periodicity of twice the unit cell. (c) EELS signal profiles of the Ti (black), O (red) and Mn (green) across the LSMO/Ti interface. The HAADF signal highlights the cell doubling effect.

Figure 2a shows the EELS signal intensities of the Au  $M_{4,5}$ , O K and Mn  $L_{2,3}$  edges across the LSMO/Au interface, in addition to the HAADF signal intensity (blue) for comparison. A small degree of intermixing is apparent at the interface but is ascribed to the data deriving from the projection through a rough interface, in addition to possible beam-broadening effects. Whilst the LSMO is unaffected by the deposition of a gold contact, a dramatic effect is observed following the deposition of Ti and explains the quenched magnetisation indicated in figure 2g. A HAADF image is given in figure 2b where the LSMO now appears bright with respect to the Ti. A clear cell-doubling effect is observed in the LSMO layer, which is consistent with a phase change to a brownmillerite structure [7,8]. The dark planes in figure 2b, highlighted by the red arrows, coincide with the  $MnO_2$  planes of the LSMO, indicating a deficiency in either manganese or oxygen. EELS was subsequently carried out to determine the origin of the phase change in the LSMO and results are summarised in figure 2c. It is immediately clear that the oxygen signal extends some distance into the Ti capping layer, decaying at a slower rate than the Mn at the interface. This indicates that the Ti acts as an oxygen getter and subsequently forms a  $TiO_x$  phase at the interface, consistent with an analysis of the Ti  $L_{2,3}$  ELNES spectrum (not shown) [9]. These results can account for the complete loss of magnetisation in the LSMO since the sensitivity of LSMO magnetisation to structural defects and oxygen deficiency is well known [10].

In the next set of experiments, we explore the effect of Ti thickness on the magnetic properties of LSMO. Figure 3a illustrates that complete quenching of the LSMO magnetisation occurs for just 1 nm of Ti. What is interesting is that the crystal structure of the LSMO appears completely intact, as illustrated in figure 3b. Nevertheless, EELS reveals substantial oxygen deficiencies,

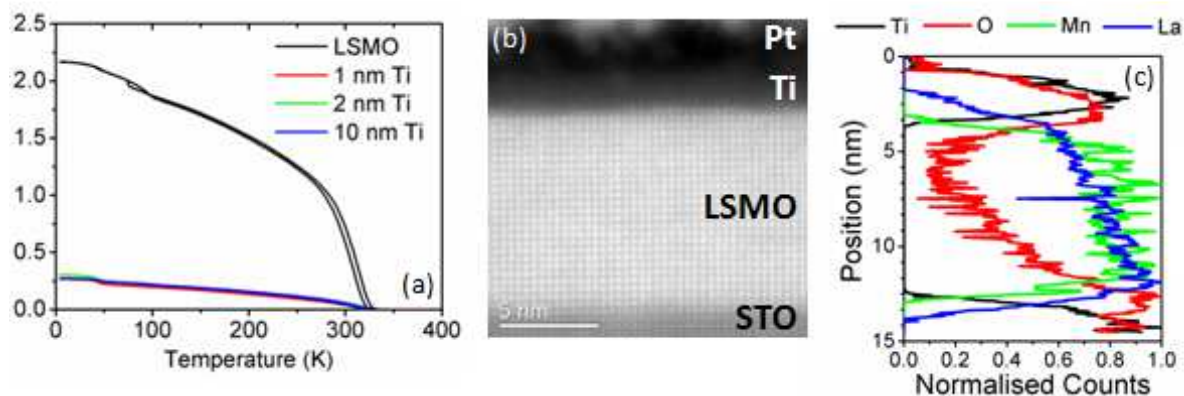


**Figure 3.** (a) SQUID measurements of Ti capping layers of different thicknesses. (b) STEM image of an LSMO film with a 1 nm thick Ti cap. (c) Corresponding EELS profiles of Ti, O, Mn and La signals across the film in (b) where the LSMO is oxygen (red) depleted.

indicating that the LSMO is able to support a significant number of oxygen vacancies prior to reconstruction. The data presented in figure 3c show the Ti  $L_{2,3}$ , O K, Mn  $L_{2,3}$  and La  $M_{4,5}$  intensity profiles across the LSMO layer following the deposition of ~1 nm of Ti. It may be observed that there is a significant oxygen signal (red line) in the Ti layer, whilst the LSMO layer is substantially oxygen depleted, suggesting an interfacial reaction and transfer of oxygen from LSMO to Ti, with the oxygen deficiency becoming more pronounced towards the Ti interface.

#### 4. Discussion and Conclusions

Given that Ti and Cr are often used as adhesion layers for noble metal electrical contacts, these results indicate that great care must be taken to protect oxygen sensitive materials from damage. Whilst an interfacial reaction is commonly exploited to improve the adhesion of ohmic contacts in microelectronic devices, it is clear that in the case of functional oxides such as LSMO, that reaction can have a detrimental effect on functionality. A suitable candidate for use as a protective barrier sandwiched between LSMO and Ti was found to be the electrically conductive perovskite oxide  $\text{SrRuO}_3$ . Alternatively, we found that  $\text{SrTiO}_3$  could also be used as a suitable mask for subsequent dry etching if an ohmic contact is not required; these results will be described elsewhere. The results presented here provide valuable insight into the effects of metal contacting and ultimately enhance our understanding towards the development of multifunctional oxide devices.

#### Acknowledgements

This work was funded by EU's 7th framework Program IFOX (NMP3-LA-2010 246102) and the Engineering and Physical Sciences research council (EPSRC) of the UK (EP/I00419X/1). Original data files relating the work presented are available at: <http://dx.doi.org/10.5525/gla.researchdata.193>.

#### 5. References

- [1] Hwang H Y, Iwasa Y, Kawasaki M, Keimer B, Nagaosa N and Y. Tokura 2012 *Nature Mater.* **11** 103
- [2] Czeschka F D, Dreher L, Brandt M S, Weiler M, Althammer M, Imort I-M, Reiss G, Thomas A, Schoch W, Limmer W, Huebl H, Gross R and Goennenwein S T B 2011 *Phys. Rev. Lett.* **107** 046601
- [3] Willmott P R and Huber J R 2000 *Rev. Mod. Phys.* **71** 315
- [4] Neave J H and Joyce B A, Dobson P J, Norton N 1983 *Appl. Phys. A* **31** 1.
- [5] Scott J, Thomas P J, MacKenzie M, McFadzean S, Wilbrink J, Craven A J and Nicholson W A P 2008 *Ultramicroscopy* **108** 1586
- [6] Hunt J A and Williams D B 1991 *Ultramicroscopy* **38** 47
- [7] Rossell M D, Lebedev O I, Van Tendeloo G, Hayashi N, Terashima T and Takano M 2004 *J. Appl. Phys.* **95** 5145
- [8] Klenov D O, Donner W, Foran B, Stemmer S 2003 *Appl. Phys. Lett.* **82** 3427
- [9] Stoyanov E, Langenhorst F, Steinle-Neumann G 2007 *American Mineralogist* **92** 577
- [10] Schumacher D, Steffen A, Voigt J, Schubert J, Brückel Th, Ambaye H and Lauter V 2013 *Phys. Rev. B* **88** 14427